A method for disentangling El Niño–mean state interaction

Masahiro Watanabe[1] and Andrew T. Wittenberg[2]

Received 13 April 2012; revised 12 June 2012; accepted 14 June 2012; published 21 July 2012.

[1] The amplitude of the El Niño-Southern Oscillation (ENSO) is known to fluctuate in long records derived from observations and general circulation models (GCMs), even when driven by constant external forcings. This involves an interaction between the ENSO cycle and the background mean state, which affects the climatological precipitation over the eastern equatorial Pacific. The changes in climatological rainfall may be ascribed to several factors: changes in mean sea surface temperature (SST), changes in SST variability, and changes in the sensitivity of precipitation to SST. We propose a method to separate these effects in model ensembles. A case study with a single GCM demonstrates that the method works well, and suggests that each factor plays a role in changing mean precipitation. Applying the method to 16 pre-industrial control simulations archived in the Coupled Model Intercomparison Project phase 5 (CMIP5) reveals that the inter-model diversity in mean precipitation arises mostly from differences in the mean SST and atmospheric sensitivity to SST, rather than from differences in ENSO amplitude. **Citation:** Watanabe, M., and A. T. Wittenberg (2012), A method for disentangling El Niño–mean state interaction, *Geophys. Res. Lett.*, *39*, L14702, doi:10.1029/2012GL052013.

1. Introduction

[2] Realistic simulation of the El Niño-Southern Oscillation (ENSO) phenomenon using coupled general circulation models (GCMs) is of great importance for predicting ENSO and evaluating its impact on global weather. The ability to simulate an ENSO with properties (amplitude, periodicity, spatial structure, phase asymmetry, etc.) close to observations is a good test of a GCM. Despite improved ENSO simulations [*AchutaRao and Sperber*, 2006], there was a large diversity in ENSO properties among the state of the art GCMs included in the Coupled Model Intercomparison Project phase 3 (CMIP3) [*Guilyardi et al.*, 2009; *Vecchi and Wittenberg*, 2010]. Errors in coupled feedback processes [*Collins et al.*, 2010; *Philip et al.*, 2010; *Lloyd et al.*, 2011] are probably the major cause of the diversity of ENSO amplitudes among GCMs and are not yet solved in CMIP5 (E. Guilyardi et al., A first look at ENSO in CMIP5, submitted to *CLIVAR Exchanges*, 2012). However, the nonlinear nature of the coupled system makes it difficult to clarify how the error in a particular process affects ENSO and the mean state. In addition, intrinsic modulation can contribute to uncertainties in ENSO properties diagnosed from centennial and shorter records, such as the observed instrumental record and many climate simulations [*Wittenberg*, 2009].

[3] ENSO is known to interact with other phenomena on a variety of time scales: the annual cycle [*Jin et al.*, 1994; *Guilyardi*, 2006], atmospheric disturbances [*Vecchi et al.*, 2006; *Jin et al.*, 2007], and decadal variability [*An and Wang*, 2000; *Choi et al.*, 2009], all of which also affect the mean state. Here, we loosely define the 'mean state' as a time average spanning a period much longer than ENSO's interannual time scale. Changes in this background mean state can affect the growth rate and frequency of El Niño/La Niña, as has been clarified using a hierarchy of models [*Jin*, 1997; *Fedorov and Philander*, 2001; *Wittenberg*, 2002]. ENSO can also feed back onto the mean state: El Niño exhibits a different spatial pattern of SST anomalies (SSTAs) than does La Niña, leading to a net warming of the eastern equatorial Pacific and cooling of the western Pacific during active ENSO epochs [*An and Jin*, 2004; *McPhaden et al.*, 2011]. Climate variables having a skewed probability distribution, such as precipitation, also exhibit mean state changes in response to changes in ENSO amplitude [*Watanabe et al.*, 2011].

[4] To improve understanding of ENSO in complex GCMs, it is necessary to devise useful metrics and methods for evaluating ENSO (Guilyardi et al., submitted manuscript, 2012). Until now, there has been no simple method to isolate the ENSO feedback effect on changes in the tropical Pacific mean state. Here we propose such a method, using monthly time series of precipitation and SST from a sufficiently long simulation or an ensemble of simulations.

2. Method and Model Ensembles

[5] The precipitation (P) over the tropical region depends nonlinearly on the underlying SST (T) [*Graham and Barnett*, 1987]. The climatological mean precipitation $\bar{P}$ can be expressed as:

$$\begin{aligned}\bar{P} &= \int\int p(P,T)dPdT \\ &= \int\int p(T)p(P|T)dPdT, \\ &= \int f(T)C(T)dT\end{aligned} \tag{1}$$

where $p(X)$ denotes the probability distribution of X, f is the probability density function (PDF) of T, and $C(T)$ is the composite of P with respect to T. In principle, the expression (1), hereafter referred to as the PDF method, holds exactly everywhere, regardless of the degree of correlation or causal linkage between P and T. The method is most helpful when the two variables are correlated, have a nonlinear relationship, and/or have different distributions, making them difficult to analyze with simpler methods.

[1]Atmosphere and Ocean Research Institute, University of Tokyo, Kashiwa, Japan.
[2]NOAA Geophysical Fluid Dynamics Laboratory, Princeton, USA.

Corresponding author: M. Watanabe, Atmosphere and Ocean Research Institute, University of Tokyo, Kashiwa, Chiba 277-8568, Japan. (hiro@aori.u-tokyo.ac.jp)

0094-8276/12/2012GL052013

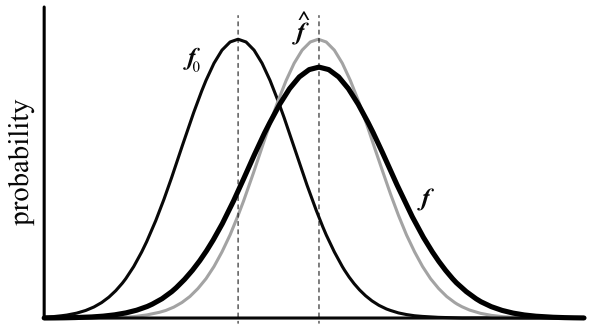

Figure 1. Schematic of the SST PDF and its decomposition. $\hat{f}$ has the same shape as f_0, but the mean of the PDF follows that of f.

[6] Given an ensemble of realizations (e.g. from different models, or different forcing scenarios), we may define references, denoted as $\bar{P}_0$, C_0, and f_0, and derive an equation for deviations from them ()′;

$$\bar{P} - \bar{P}_0 = \int f' C_0(T) dT + \int f_0 C'(T) dT + \int f' C'(T) dT, \quad (2)$$

where C_0 represents the typical shape of the precipitation composite and is obtained from the ensemble average of $C(T)$, i.e., $C_0 \equiv \langle C(T) \rangle$. At extreme values of T, the C_0 defined this way will be representative of only one or two models, but fortunately those extreme values of T are, by definition, rarely visited by the models. We have further assumed that wherever $f = 0$, i.e. at those values of T not sampled by the ensemble member, C can be approximated as C_0, such that $C' = 0$ at those values of T. The reference PDF f_0 is defined as $f_0 \equiv \langle f(T - \bar{T} + \langle \bar{T} \rangle) \rangle$, where $\bar{T}$ is the annual-mean climatology of T and $\langle \bar{T} \rangle$ is the ensemble average, to represent the plausible mean shape of the PDF while sharing the mean position with $\langle f \rangle$. $\bar{P}_0$ is expressed as $\bar{P}_0 \equiv \int f_0 C_0(T) dT$, so that the left hand side denotes the excess mean precipitation in a single ensemble member. The reference mean precipitation is slightly different from $\langle \bar{P} \rangle$, but the difference is about 5% and negligible for the results presented in the next section. The first term on the right hand side of (2) captures the impact of a member's difference in SST PDF on $\bar{P}$, given the reference sensitivity of P to T. The second term, which captures the impact of a member's different sensitivity of P to T, given the reference PDF of T, is called the precipitation sensitivity effect. The third term, which represents nonlinear impacts on $\bar{P}$, is small in most of the cases that we have tested. Here we apply (2) to the Niño 3 region (150° W–90° W, 5° S–5° N), so that the monthly time series of the Niño 3-averaged SST and precipitation are used for the analysis. The composite of P is computed using a Niño 3 SST bin width of 0.2 K. There is a slight westward shift in the maximum location of the SSTA variability in several CMIP5 models that we have analyzed, but it is not critical for the choice of the region.

[7] A similar method has been used in cloud regime analysis, where cloud amounts are sorted by mid-tropospheric vertical velocity [*Bony et al.*, 2004; *Bony and Dufresne*, 2005]. In the present application, one has to be careful when interpreting the term involving f' since it includes not only the change in ENSO properties, but also biases or changes in mean SST and the seasonal cycle. The first term in (2) can therefore be decomposed as

$$\int f' C_0(T) dT = \int (f - \hat{f}) C_0(T) dT + \int (\hat{f} - f_0) C_0(T) dT, \quad (3)$$

where $\hat{f}$ has the shape of f_0 but the mean $\bar{T}$ of f (Figure 1). The first term on the right hand side represents the effect of the change in the shape of the SST PDF, typically associated with an ENSO amplitude difference; we shall refer to it as the ENSO SSTA amplitude effect. The second term indicates the effect of the change in mean SST. While the difference in PDF shape, $f - \hat{f}$, is affected by the seasonal cycle, we confirmed that the results did not change much when the seasonal cycle was removed from T in advance (see discussion). Since the mean SST can be changed by either model biases or external forcing, the magnitude and impact of the mean SST effect will depend on the ensemble.

[8] We demonstrate the evaluation of the ENSO SSTA amplitude effect with two types of model ensembles. One is a four-member ensemble from the Model for Interdisciplinary Research on Climate version 5 (MIROC5) [*Watanabe et al.*, 2010]. Each member consists of a 100-year pre-industrial control run, with slightly different values of an entrainment parameter in the cumulus convection scheme. The ensemble spans a wide range of ENSO amplitudes from 0.61 to 1.63 K [*Watanabe et al.*, 2011]. The other ensemble is the multi-model ensemble (MME) of the CMIP5, which is only partly available as of this writing [*Taylor et al.*, 2011]. We use pre-industrial control runs from 16 different models (Table 1). The length of each CMIP5 run differs, but the statistics in (2)–(3) are calculated using all available data.

3. Results

[9] Figure 2 summarizes the results of the PDF method applied to the MIROC5 ensemble. The ENSO amplitude systematically increases from one experiment (L575) to the other (L500), the latter showing a positively skewed SST PDF (Figure 2a). The shape of $C(T)$ is similar for all the

Table 1. List of the CMIP5 Models and the Integration Length of the Pre-industrial Control Experiments

Model Number	Model Name	Integration Years
1	GISS-E2-R	850
2	INM-CM4	450
3	MRI-CGCM3	200
4	CSIRO Mk-3.6	500
5	GISS-E2-H	1106
6	IPSL-CM5A-LR	800
7	IPSL-CM5A-MR	300
8	GFDL-ESM2G	500
9	MIROC5	500
10	MPI-ESM-LR	1000
11	HadGEM2-CC	240
12	CNRM-CM5	850
13	CanESM2	996
14	NorESM1-M	500
15	GFDL-CM3	500
16	GFDL-ESM2M	500

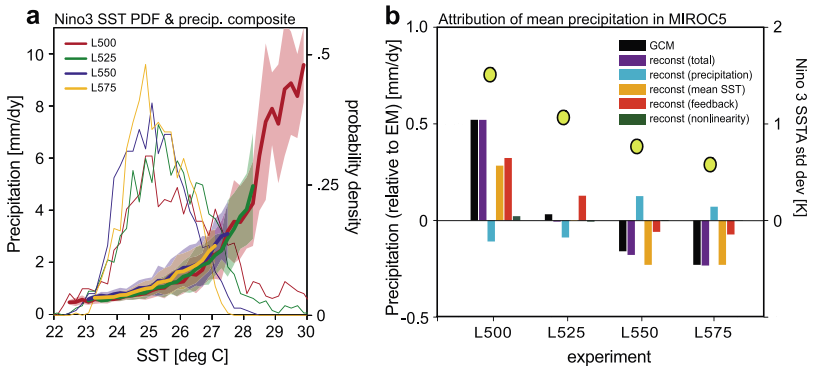

Figure 2. (a) PDFs of the Niño 3 SST (thin curves) and associated composites of the Niño 3 precipitation (thick curves, mm day^{-1}) in the four experiments by MIROC5. The shading indicates std dev of the composite. (b) Reconstruction of the mean Niño 3 precipitation, the reference value subtracted, following equations (2)–(3): total reconstruction (purple), precipitation sensitivity (blue), mean SST effect (orange), ENSO amplitude feedback (red), and nonlinearity (green), respectively. The reference values obtained from the GCMs (black bars) are also presented. The std dev of the Niño 3 SST anomaly ($\sigma_{\text{niño}}$, K) is shown by yellow circles. The names of the experiments follow *Watanabe et al.* [2011].

members, but the tail of intense precipitation extends as ENSO becomes stronger. The reconstruction of the Niño 3 mean precipitation, $\bar{P}_{\text{niño}}$, is successful by definition (black and purple bars in Figure 2b). The decomposition of the total reconstruction into four components shows that in terms of the impact on mean precipitation, the change in ENSO SSTA amplitude (red bars) can be as important as the change in mean SST (orange bars). The change in precipitation sensitivity, which one might think of as being more directly affected by changes in convection parameters, here acts to counteract the change in $\bar{P}_{\text{niño}}$ (blue bars). This result is consistent with the arguments in *Watanabe et al.* [2011].

[10] Before presenting the results for the CMIP5 MME, the ensemble-mean precipitation and its diversity are shown in Figure 3. A preliminary analysis of the mean precipitation fields reveals that the pattern is not significantly improved over the CMIP3 MME (N. Hirota, personal communication, 2012), and still suffers from a double-ITCZ bias [*Bellucci et al.*, 2010]. The spread among the 16 models (shading) indicates that the inter-model differences are especially large over the dry zones of the continents, subtropical oceans, and equatorial Pacific.

[11] Unlike the previous example, the PDFs of T in CMIP5 models are shifted relative to each other, representing biases in mean SST (Figure 4a). The shape of $C(T)$ is also different across the models, especially at higher values of SST (Figure 4b). Figure 4c shows the reconstruction of $\bar{P}_{\text{niño}}$ for the 16 models, ordered following the ENSO amplitude. The diversity in $\bar{P}_{\text{niño}}$ exceeds 3 mm day^{-1} and is well reproduced by the PDF method. In contrast to the parameter ensemble shown in Figure 2, the ENSO SSTA amplitude feedback, highly correlated with the ENSO amplitude (r = 0.75), is much smaller in the MME (red bars). $\bar{P}_{\text{niño}}$ is roughly explained by the two effects in (2)–(3), which are not unique; a different shape of $C(T)$ revealed in Figure 4b is critical in some models (*e.g.*, 2, 3, 11, 14, and 16) whereas the mean SST difference is critical in others (*e.g.*, 1, 4, 8, 12, and 13). Models showing that each term is very close to the ensemble mean (9 and 15) do not imply that they are "best," since the ensemble mean $\bar{P}_{\text{niño}}$ itself has a positive error of 0.5 mm day^{-1} relative to the 1979–2009 observation, due to overestimation of $C(T)$ for T < 28°C (cf. black curve in Figure 4b). The model 9 is identical to one of the parameter setting in another model ensemble shown in Figure 2, but

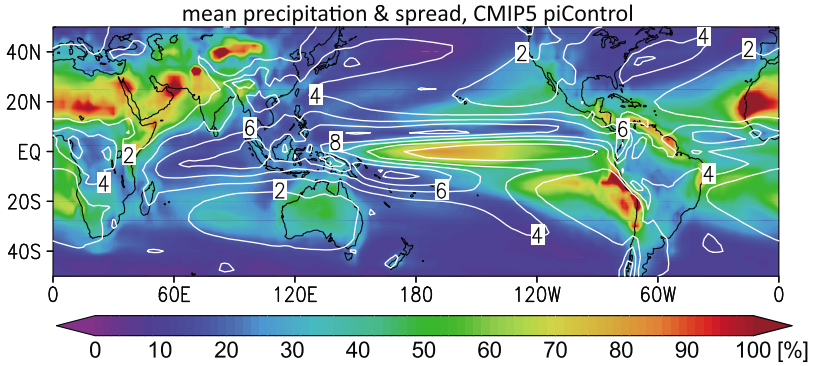

Figure 3. Multi-model ensemble mean of $\bar{P}$ (contour, mm day^{-1}) and the inter-model spread scaled by the ensemble mean (shading, %) obtained from the pre-industrial control runs by 16 CMIP5 models.

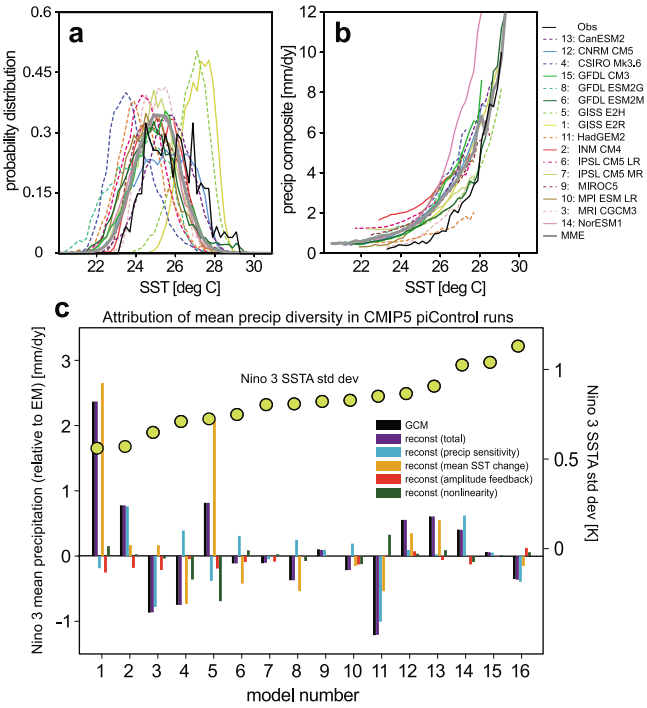

Figure 4. As in Figure 2 but for 16 pre-industrial runs by CMIP5 models. The model number, sorted by $\sigma_{niño}$, is listed in Table 1. The decomposition uses (2) and (3). In (a)–(b), observations (Global Precipitation Climatology Project version 2 data by *Adler et al.* [2003] and monthly SST data by *Ishii et al.* [2006], both for 1979–2009) are also plotted by black curves.

the contribution of each term is not the same since the excess mean precipitation changes the sign and magnitude in different ensembles.

4. Summary and Discussion

[12] We have shown that the PDF equations (2) and (3) work well in decomposing $\bar{P}_{niño}$ simulated in GCMs. The ENSO SSTA amplitude feedback works to increase $\bar{P}_{niño}$ due to asymmetry in the precipitation response to T. However, the relative importance of this term varies. In the parameter ensemble examined here from a single GCM, changes in $\bar{P}_{niño}$ are largely attributable to changes in both mean SST and SSTA amplitude. Given that $\bar{P}_{niño}$ can measure ENSO stability [*Watanabe et al.*, 2011; *Kim et al.*, 2011], a two-way feedback could conceivably contribute to low-frequency modulation of both ENSO and the mean state. In contrast, for the CMIP5 MME where models differ structurally in many aspects (dynamical core, physical parameterization scheme, and resolution), inter-model differences in $\bar{P}_{niño}$ are explained mainly by differences in mean SST, and by different sensitivities of precipitation to SST.

[13] We have also tried defining f to be the PDF of the SSTA in (1). In this case, the first term in (2) cleanly represents just the ENSO SSTA amplitude influence on the mean precipitation. The second term then includes impacts of the change in mean SST on the precipitation response to SSTAs, which in the CMIP5 MME is larger than the impact of ENSO SSTA amplitude differences (Figure 4). To estimate the SSTA amplitude impact on mean rainfall in an ensemble with large SST biases, it would be better to define f be the SSTA; however, the results are similar to those presented above. For example, the precipitation sensitivity effects (second term in (2)) in the CMIP5 MME are highly correlated (r = 0.95) with the corresponding term when we use Niño3 SSTA to define f.

[14] The PDF method has a potential for other applications. For example, one can use surface wind stresses instead of precipitation to understand causes of the diversity in the mean dynamical fields in the CMIP5 MME. Another application is to use a long, single-member integration [e.g., *Wittenberg*, 2009]. The ensemble mean can be replaced by the long-term mean, while the deviation is defined using a particular epoch. The evaluation of MME can also be done by using observations to define f_0 and $C_0(T)$.

[15] The PDF method could be extended to decompose T into $\bar{T}$, mean seasonal cycle, and anomalies. While the isolation of the seasonal cycle was not crucial in the present analysis, for some applications there might be an interaction among the mean state, seasonal cycle, and ENSO [*Guilyardi*, 2006]. The asymmetric nature of ENSO can also modify $\bar{P}$ through changing $\bar{T}$ [*An and Jin*, 2004]. Thus, our method should ultimately disentangle the impacts of changing variance and skewness of ENSO on the mean precipitation and SST.

[16] **Acknowledgments.** M.W. is grateful to F.-F. Jin for stimulating discussion. Thanks are also due to M. Collins, J.-S. Kug, J. N. Brown, and an anonymous reviewer for their comments. This work was supported by the Innovative Program of Climate Change Projection for the 21st Century from MEXT, Japan, and the Mitsui Environment Fund C-042.

[17] The Editor thanks the two anonymous reviewers for their assistance in evaluating this paper.

References

AchutaRao, K., and K. Sperber (2006), ENSO simulations in coupled ocean-atmosphere models: Are the current models better? *Clim. Dyn.*, *27*, 1–15, doi:10.1007/s00382-006-0119-7.

Adler, R. F., et al. (2003), The version 2 Global Precipitation Climatology Project (GPCP) monthly precipitation analysis (1979–present), *J. Hydrometeorol.*, *4*, 1147–1167, doi:10.1175/1525-7541(2003)004<1147:TVGPCP>2.0.CO;2.

An, S.-I., and F.-F. Jin (2004), Nonlinearity and asymmetry of ENSO, *J. Clim.*, *17*, 2399–2412, doi:10.1175/1520-0442(2004)017<2399:NAAOE>2.0.CO;2.

An, S.-I., and B. Wang (2000), Interdecadal change of the structure of the ENSO mode and its impact on the ENSO frequency, *J. Clim.*, *13*, 2044–2055, doi:10.1175/1520-0442(2000)013<2044:ICOTSO>2.0.CO;2.

Bellucci, A., S. Gualdi, and A. Navarra (2010), The double-ITCZ syndrome in coupled general circulation models: The role of large-scale vertical circulation regimes, *J. Clim.*, *23*, 1127–1145, doi:10.1175/2009JCLI3002.1.

Bony, S., and J. L. Dufresne (2005), Marine boundary layer clouds at the heart of tropical cloud feedback uncertainties in climate models, *Geophys. Res. Lett.*, *32*, L20806, doi:10.1029/2005GL023851.

Bony, S., J.-L. Dufresne, H. LeTreut, J.-J. Morcrette, and C. Senior (2004), On dynamic and thermodynamic components of cloud changes, *Clim. Dyn.*, *22*, 71–86, doi:10.1007/s00382-003-0369-6.

Choi, J., S.-I. An, B. Dewitte, and W. M. Hsieh (2009), Interactive feedback between the tropical Pacific decadal oscillation and ENSO in a coupled general circulation model, *J. Clim.*, *22*, 6597–6611, doi:10.1175/2009JCLI2782.1.

Collins, M., et al. (2010), The impact of global warming on the tropical Pacific Ocean and El Niño, *Nat. Geosci.*, *3*, 391–397, doi:10.1038/ngeo868.

Fedorov, A. V., and S. G. Philander (2001), A stability analysis of tropical ocean–atmosphere interactions: Bridging measurements and theory for El Niño, *J. Clim.*, *14*, 3086–3101, doi:10.1175/1520-0442(2001)014<3086:ASAOTO>2.0.CO;2.

Graham, N. E., and T. P. Barnett (1987), Sea surface temperature, surface wind divergence, and convection over tropical oceans, *Science*, *238*, 657–659, doi:10.1126/science.238.4827.657.

Guilyardi, E. (2006), El Niño–mean state–seasonal cycle interactions in a multi-model ensemble, *Clim. Dyn.*, *26*, 329–348, doi:10.1007/s00382-005-0084-6.

Guilyardi, E., et al. (2009), Understanding El Niño in ocean-atmosphere general circulation models: Progress and challenges, *Bull. Am. Meteorol. Soc.*, *90*, 325–340, doi:10.1175/2008BAMS2387.1.

Ishii, M., M. Kimoto, K. Sakamoto, and S. Iwasaki (2006), Steric sea level changes estimated from historical ocean subsurface temperature and salinity analyses, *J. Oceanogr.*, *62*, 155–170, doi:10.1007/s10872-006-0041-y.

Jin, F. F. (1997), An equatorial ocean recharge paradigm for ENSO. Part II: A stripped-down coupled model, *J. Atmos. Sci.*, *54*, 830–847, doi:10.1175/1520-0469(1997)054<0830:AEORPF>2.0.CO;2.

Jin, F.-F., J. D. Neelin, and M. Ghil (1994), El Niño on the devil's staircase: Annual subharmonic steps to chaos, *Science*, *264*, 70–72, doi:10.1126/science.264.5155.70.

Jin, F.-F., L. Lin, L. A. Timmermann, and J. Zhao (2007), Ensemble-mean dynamics of the ENSO recharge oscillator under state-dependent stochastic forcing, *Geophys. Res. Lett.*, *34*, L03807, doi:10.1029/2006GL027372.

Kim, D., Y.-S. Jang, D.-H. Kim, Y.-H. Kim, M. Watanabe, F.-F. Jin, and J.-S. Kug (2011), El Niño–Southern Oscillation sensitivity to cumulus entrainment in a coupled general circulation model, *J. Geophys. Res.*, *116*, D22112, doi:10.1029/2011JD016526.

Lloyd, J., E. Guilyardi, and J. Weller (2011), The role of atmosphere feedbacks during ENSO in the CMIP3 models. Part II: using AMIP runs to understand the heat flux feedback mechanisms, *Clim. Dyn.*, *37*, 1271–1292, doi:10.1007/s00382-010-0895-y.

McPhaden, M. J., T. Lee, and D. McClurg (2011), El Niño and its relationship to changing background conditions in the tropical Pacific Ocean, *Geophys. Res. Lett.*, *38*, L15709, doi:10.1029/2011GL048275.

Philip, S. Y., M. Collins, G. J. van Oldenborgh, and B. J. J. M. van den Hurk (2010), The role of atmosphere and ocean physical processes in ENSO in a perturbed physics coupled climate model, *Ocean Sci.*, *6*, 441–459, doi:10.5194/os-6-441-2010.

Taylor, K. E., R. J. Stouffer, and G. A. Meehl (2011), An overview of CMIP5 and the experiment design, *Bull. Am. Meteorol. Soc.*, *93*, 485–498, doi:10.1175/BAMS-D-11-00094.1.

Vecchi, G. A., and A. T. Wittenberg (2010), El Niño and our future climate: Where do we stand?, *Clim. Change*, *1*, 260–270, doi:10.1002/wcc.33.

Vecchi, G. A., A. T. Wittenberg, and A. Rosati (2006), Reassessing the role of stochastic forcing in the 1997–8 El Niño, *Geophys. Res. Lett.*, *33*, L01706, doi:10.1029/2005GL024738.

Watanabe, M., et al. (2010), Improved climate simulation by MIROC5: Mean states, variability, and climate sensitivity, *J. Clim.*, *23*, 6312–6335, doi:10.1175/2010JCLI3679.1.

Watanabe, M., M. Chikira, Y. Imada, and M. Kimoto (2011), Convective control of ENSO simulated in MIROC5, *J. Clim.*, *24*, 543–562, doi:10.1175/2010JCLI3878.1.

Wittenberg, A. T. (2002), ENSO response to altered climates, PhD thesis, 475 pp., Princeton Univ., Princeton, N. J.

Wittenberg, A. T. (2009), Are historical records sufficient to constrain ENSO simulations?, *Geophys. Res. Lett.*, *36*, L12702, doi:10.1029/2009GL038710.